



FREE AND FORCED VIBRATION OF REISSNER–MINDLIN PLATES WITH FREE EDGES RESTING ON ELASTIC FOUNDATIONS

H.-S. SHEN, J. YANG AND L. ZHANG

School of Civil Engineering and Mechanics, Shanghai Jiao Tong University, 1954 Hua Shan Road, Shanghai 200030, People's Republic of China. E-mail: hsshenn@mail1.sjtu.edu.cn

(Received 18 May 2000, and in final form 20 October 2000)

Free and forced vibration analysis is presented for Reissner–Mindlin plates with four free edges resting on a Pasternak-type elastic foundation. The formulations are based on the Reissner–Mindlin plate theory, considering the first order shear deformation effect and including the plate–foundation interaction and thermal effects. A new set of admissible functions, which satisfy both geometrical and natural boundary conditions, are developed for the free vibration analysis of moderately thick plates with four free edges. The Rayleigh–Ritz Method is employed in conjunction with this set of admissible functions to determine the vibration behaviors. Then on this basis, the modal superposition approach is used in conjunction with Mindlin–Goodman procedure to determine the dynamic response of free edge Reissner–Mindlin plates exposed to thermomechanical loading. The mechanical loads consist of transverse partially distributed impulsive loads and in-plane edge loads while the temperature field is assumed to exhibit a linear variation through the thickness of the plate. The numerical illustrations concern moderately thick plates with four free edges resting on Pasternak-type elastic foundations with the Winkler elastic foundations being a limiting case. Effects of foundation stiffness, transverse shear deformation, plate aspect ratio, shape and duration of impulsive load, loaded area, and initial membrane stress as well as thermal bending stress on the dynamic response of Reissner–Mindlin plates are studied.

© 2001 Academic Press

1. INTRODUCTION

Dynamic response of simply supported, moderately thick rectangular plates under transverse partially distributed impulsive loads combined with in-plane edge loads and temperature field and resting on a Pasternak-type elastic foundation was the subject of a recent investigation [1]. The analysis was based on the Reissner–Mindlin first order shear deformation plate theory (FSDPT). Dynamic response was determined by using both the modal superposition approach (MSA) and state variable approach (SVA). Such solutions may find important applications in stress analysis and design of concrete pavements of airfields.

Many publications have appeared in the literature on the free or forced vibration of isotropic and composite laminated thick plates. The dynamic response of plates are presented mainly for a few edge boundary conditions, such as those simply supported at four edges (Navier-type solutions) or at two parallel edges (Levy-type solutions). For other type of boundary conditions, only numerical results can be found [2–5], and most of them are for the free vibration analysis. The Rayleigh–Ritz method has been frequently applied and it should select appropriate admissible functions (e.g. beam vibration mode shapes [6]) representing the deflection of the plate under consideration. However, as mentioned by

Bassily [7] and Dawe [8], this kind of admissible function for the plate involving one or more free edges is less satisfactory in free vibration analysis. Consequently, some modified functions, e.g. degenerated beam functions [9], orthogonal polynomials [10, 11], pb-2 type polynomial function [12], are introduced to overcome this difficulty, but they do not satisfy natural boundary conditions and thus show slow convergence. Moreover, Gorman [13] and Gorman and Ding [14] employed the superposition method to obtain accurate free vibration solutions for completely free rectangular thin or thick plates. Shen [15, 16] gave the analytical solutions for non-linear bending of Reissner–Mindlin plates with four free edges subjected to transverse partially distributed loads combined with temperature field or in-plane loads and resting on elastic foundations.

The present study extends the previous work [1] to the case of moderately thick rectangular plates with four free edges resting on a Pasternak-type elastic foundation. A new set of admissible functions, which satisfy both geometrical and natural boundary conditions, are developed for the free vibration analysis of moderately thick plates with four free edges. The Rayleigh–Ritz Method is employed in conjunction with this set of admissible functions to determine the vibration behavior. Then on this basis, the modal superposition approach in conjunction with Mindlin–Goodman procedure [17, 18], is used to determine the dynamic response of free edge Reissner–Mindlin plates exposed to thermomechanical loading. The mechanical loads consist of transverse partially distributed impulsive loads and in-plane edge loads while the temperature field is assumed to exhibit a linear variation through the thickness of the plate. The material properties are assumed to be independent of temperature. The formulations are based on Reissner–Mindlin first order shear deformation plate theory and include the plate–foundation interaction and thermal effects. Numerical examples are presented that relate to the dynamic behaviors of free edge moderately thick plates resting on Pasternak-type elastic foundations, from which results for Winkler foundations are obtained as a limiting case. Static bending is treated as a degenerated problem.

2. GOVERNING EQUATIONS AND THEIR DIMENSIONLESS FORMS

Consider a moderately thick rectangular plate of length a , width b , and thickness h , which rests on a Pasternak-type elastic foundation. The four edges of the plate are all free. A Cartesian co-ordinate system (X, Y, Z) is located at the middle plane of the plate, where X is longitudinal and Z is perpendicular to the plate. The origin point is located at the center of the plate, as shown in Figure 1. The plate is exposed to a stationary temperature field $T(X, Y, Z)$ and transverse impulsive load q over a central area $a_1 \times b_1$ combined with in-plane edge loads N_X in the X direction and N_Y in the Y direction. As is customary [15, 16, 19–21], the foundation is assumed attached to the plate and separation does not arise. The load–displacement relationship of the foundation is assumed to be $p = \bar{K}_1 \bar{W} - \bar{K}_2 \nabla^2 \bar{W}$, where \bar{W} is the plate deflection, p is the force per unit area, \bar{K}_1 is the Winkler foundation stiffness, \bar{K}_2 is a constant showing the effect of the shear interactions of the vertical elements, ∇^2 is the Laplace operator in X and Y . $\bar{\Psi}_X$ and $\bar{\Psi}_Y$ are the mid-plane rotations of the normals about the Y - and X -axis respectively, \bar{t} is the time and Ω is the frequency.

It is postulated that the temperature field $T(X, Y, Z)$ exhibits a linear variation through the plate thickness, i.e.,

$$T(X, Y, Z) = T_0 \left(1 + C \frac{Z}{h} \right), \quad (1)$$

in which T_0 and C denote the temperature amplitude and gradient respectively.

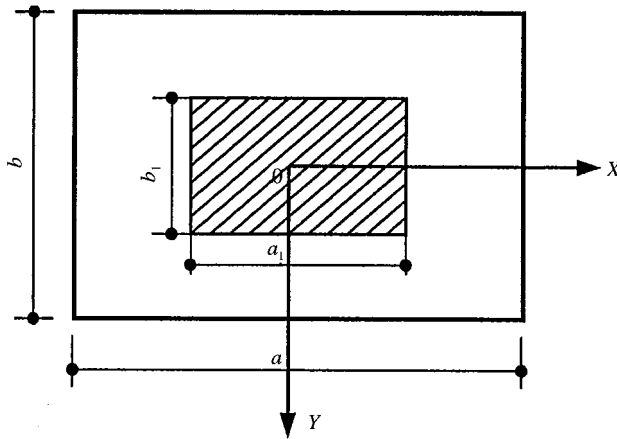


Figure 1. A Reissner-Mindlin plate subjected to a transverse partially distributed impulsive load.

The thermal moments caused by the temperature field $T(X, Y, Z)$ are defined by

$$\bar{M}^T = \frac{E\alpha}{1 - \nu} \int_{-h/2}^{h/2} ZT(X, Y, Z) dZ, \tag{2}$$

where α is the thermal expansion coefficient of a plate, E is Young’s modulus and ν is the Poisson ratio.

The deduction of the governing equations associated with Reissner-Mindlin first order shear deformation plate theory, and including the plate–foundation interaction and thermal effects, follows the same pattern as in the case of its static counterpart [15], so that the motion equations can be written as

$$L_{11}(\bar{\Psi}_X) + L_{12}(\bar{\Psi}_Y) + L_{13}(\bar{W}) - \bar{K}_1 \bar{W} + \bar{K}_2 \nabla^2 \bar{W} + q = L_{14}(\bar{W}), \tag{3}$$

$$L_{21}(\bar{\Psi}_X) + L_{22}(\bar{\Psi}_Y) + L_{23}(\bar{W}) - \bar{M}_{,x}^T = L_{24}(\bar{\Psi}_X), \tag{4}$$

$$L_{31}(\bar{\Psi}_X) + L_{32}(\bar{\Psi}_Y) + L_{33}(\bar{W}) - \bar{M}_{,y}^T = L_{34}(\bar{\Psi}_Y), \tag{5}$$

where

$$\begin{aligned} L_{11}(\) &= \kappa^2 Gh \frac{\partial}{\partial X}, & L_{12}(\) &= \kappa^2 Gh \frac{\partial}{\partial Y}, \\ L_{13}(\) &= (\kappa^2 Gh + N_X) \frac{\partial^2}{\partial X^2} + (\kappa^2 Gh + N_Y) \frac{\partial^2}{\partial Y^2}, & L_{14}(\) &= I_1 \frac{\partial^2}{\partial t^2}, \\ L_{21}(\) &= D \left(\frac{\partial^2}{\partial X^2} + \frac{1 - \nu}{2} \frac{\partial^2}{\partial Y^2} \right) - \kappa^2 Gh, & L_{23}(\) &= -\kappa^2 Gh \frac{\partial}{\partial X}, \\ L_{31}(\) = L_{22}(\) &= \frac{1 + \nu}{2} D \frac{\partial}{\partial X \partial Y}, & L_{32}(\) &= D \left(\frac{1 - \nu}{2} \frac{\partial^2}{\partial X^2} + \frac{\partial^2}{\partial Y^2} \right) - \kappa^2 Gh, \\ L_{33}(\) &= -\kappa^2 Gh \frac{\partial}{\partial Y}, & L_{34}(\) = L_{24}(\) &= I_3 \frac{\partial^2}{\partial t^2}, & \nabla^2 &= \frac{\partial^2}{\partial X^2} + \frac{\partial^2}{\partial Y^2}, \end{aligned} \tag{6}$$

in which

$$D = \frac{Eh^3}{12(1-\nu^2)} \quad (I_1, I_3) = \int_{-h/2}^{h/2} \rho(1, Z^2) dZ. \quad (7)$$

D is flexural rigidity, G is shear modulus, and ρ is the mass density of the plate. Also, κ^2 is the shear factor, which accounts for the non-uniformity of the shear strain distribution through the plate thickness. For Reissner plate theory $\kappa^2 = 5/6$ while for Mindlin plate theory $\kappa^2 = \pi^2/12$.

The stress resultants are

$$\bar{M}_X = D \left(\frac{\partial \bar{\Psi}_X}{\partial X} + \nu \frac{\partial \bar{\Psi}_Y}{\partial Y} \right) - \bar{M}^T, \quad (8)$$

$$\bar{M}_Y = D \left(\nu \frac{\partial \bar{\Psi}_X}{\partial X} + \frac{\partial \bar{\Psi}_Y}{\partial Y} \right) - \bar{M}^T, \quad (9)$$

$$\bar{M}_{XY} = \frac{(1-\nu)}{2} D \left(\frac{\partial \bar{\Psi}_X}{\partial Y} + \frac{\partial \bar{\Psi}_Y}{\partial X} \right), \quad (10)$$

$$\bar{Q}_X = \kappa^2 Gh \left(\frac{\partial \bar{W}}{\partial X} + \bar{\Psi}_X \right), \quad (11)$$

$$\bar{Q}_Y = \kappa^2 Gh \left(\frac{\partial \bar{W}}{\partial Y} + \bar{\Psi}_Y \right). \quad (12)$$

If all four edges of the plate are free, the boundary conditions are

$$X = \mp a/2:$$

$$\bar{M}_X = 0, \quad \bar{M}_{XY} = 0, \quad \bar{Q}_X = 0. \quad (13a)$$

$$Y = \mp b/2:$$

$$\bar{M}_Y = 0, \quad \bar{M}_{XY} = 0, \quad \bar{Q}_Y = 0. \quad (13b)$$

Because of equations (1) and (2), it is noted that the temperature does not vary in X and Y , then thermal moment \bar{M}^T is a constant, so that the boundary conditions of equation (13) are non-homogeneous, but in equations (4) and (5) $\bar{M}_{,x}^T = \bar{M}_{,y}^T = 0$.

Introducing dimensionless quantities (in which the alternative forms k_1 and k_2 are not needed until the numerical examples are considered),

$$x = \pi \frac{X}{a}, \quad y = \pi \frac{Y}{b}, \quad \beta = \frac{a}{b}, \quad \theta = \frac{\sqrt{12}a}{\pi h}, \quad \gamma = \frac{\pi^2 D}{a^2 \kappa^2 Gh} \quad (\nu_1, \nu_2) = \left(\frac{1-\nu}{2}, \frac{1+\nu}{2} \right),$$

$$W = \frac{\bar{W}}{h} \quad (\Psi_x, \Psi_y) = (\bar{\Psi}_X, \bar{\Psi}_Y) \frac{a}{\pi h} \quad (Q_x, Q_y) = (\bar{Q}_X, \bar{Q}_Y) \frac{a}{\pi \kappa^2 Gh^2},$$

$$(M_x, M_y, M_{xy}, M^T) = (\bar{M}_X, \bar{M}_Y, \bar{M}_{XY}, \bar{M}^T) \frac{a^2}{\pi^2 Dh} \quad (K_1, k_1) = (a^4, b^4) \frac{\bar{K}_1}{\pi^4 D},$$

$$(K_2, k_2) = (a^2, b^2) \frac{\bar{K}_2}{\pi^2 D}, \quad t = \frac{\bar{t}\pi}{a} \sqrt{\frac{E}{\rho(1-\nu^2)}}, \quad \omega^2 = \Omega^2 \frac{\rho a^2(1-\nu^2)}{\pi^2 E},$$

$$\lambda_q = \frac{qa^4}{\pi^4 D h}, \quad \lambda_x = \frac{N_X a^2}{\pi^2 D}, \quad \lambda_y = \frac{N_Y b^2}{\pi^2 D}. \tag{14}$$

Equations (3)–(5) may then be written in dimensionless form as

$$L_{11}(\Psi_x) + L_{12}(\Psi_y) + L_{13}(W) - K_1 W + K_2 \bar{V}^2 W + \lambda_q = L_{14}(W), \tag{15}$$

$$L_{21}(\Psi_x) + L_{22}(\Psi_y) + L_{23}(W) = L_{24}(\Psi_x), \tag{16}$$

$$L_{31}(\Psi_x) + L_{32}(\Psi_y) + L_{33}(W) = L_{34}(\Psi_y), \tag{17}$$

where

$$L_{11}(\) = \frac{1}{\gamma} \frac{\partial}{\partial x}, \quad L_{12}(\) = \frac{\beta}{\gamma} \frac{\partial}{\partial y}, \quad L_{13}(\) = \left(\frac{1}{\gamma} + \lambda_x\right) \frac{\partial^2}{\partial x^2} + \left(\frac{1}{\gamma} + \lambda_y \beta^2\right) \beta^2 \frac{\partial^2}{\partial y^2},$$

$$L_{14}(\) = \theta^2 \frac{\partial^2}{\partial t^2}, \quad L_{21}(\) = \left(\frac{\partial^2}{\partial x^2} + \nu_1 \beta^2 \frac{\partial^2}{\partial y^2}\right) - \frac{1}{\gamma}, \quad L_{23}(\) = -\frac{1}{\gamma} \frac{\partial}{\partial x},$$

$$L_{31}(\) = L_{22}(\) = \nu_2 \beta \frac{\partial}{\partial x \partial y}, \quad L_{32}(\) = \left(\nu_1 \frac{\partial^2}{\partial x^2} + \beta^2 \frac{\partial^2}{\partial y^2}\right) - \frac{1}{\gamma}, \quad L_{33}(\) = -\frac{\beta}{\gamma} \frac{\partial}{\partial y},$$

$$L_{34}(\) = L_{24}(\) = \frac{\partial^2}{\partial t^2}, \quad \bar{V}^2 = \frac{\partial^2}{\partial x^2} + \beta^2 \frac{\partial^2}{\partial y^2} \tag{18}$$

and the dimensionless forms of stress resultants become

$$M_x = \frac{\partial \Psi_x}{\partial x} + \nu \beta \frac{\partial \Psi_y}{\partial y} - M^T, \tag{19}$$

$$M_y = \nu \frac{\partial \Psi_x}{\partial x} + \beta \frac{\partial \Psi_y}{\partial y} - M^T, \tag{20}$$

$$M_{xy} = \nu_1 \left(\beta \frac{\partial \Psi_x}{\partial y} + \frac{\partial \Psi_y}{\partial x} \right), \tag{21}$$

$$Q_x = \frac{\partial W}{\partial x} + \Psi_x, \quad Q_y = \beta \frac{\partial W}{\partial y} + \Psi_y. \tag{22, 23}$$

The boundary conditions of equation (13) become

$$x = \mp \pi/2: \quad M_x = 0, \quad M_{xy} = 0, \quad Q_x = 0. \tag{24a}$$

$$y = \mp \pi/2: \quad M_y = 0, \quad M_{xy} = 0, \quad Q_y = 0 \tag{24b}$$

and zero initial conditions are assumed, i.e.

$$(W, \Psi_x, \Psi_y)|_{t=0} = 0 \quad \left(\frac{\partial W}{\partial t}, \frac{\partial \Psi_x}{\partial t}, \frac{\partial \Psi_y}{\partial t} \right) \Big|_{t=0} = 0. \tag{25}$$

3. FREE VIBRATION ANALYSIS

3.1. ENERGY FUNCTIONAL

The strain energy for initially stressed Reissner–Mindlin plates may be written in the dimensionless form as [19]

$$U = \frac{1}{2} \int_{-\pi/2}^{\pi/2} \int_{-\pi/2}^{\pi/2} \left\{ \left(\frac{\partial \Psi_x}{\partial x} \right)_2 + \beta^2 \left(\frac{\partial \Psi_y}{\partial y} \right)^2 + 2\nu\beta \frac{\partial \Psi_x}{\partial x} \frac{\partial \Psi_y}{\partial y} + \frac{1-\nu}{2} \left(\beta \frac{\partial \Psi_x}{\partial y} + \frac{\partial \Psi_y}{\partial x} \right)^2 + \frac{1}{\gamma} \left[\left(\Psi_x + \frac{\partial W}{\partial x} \right)^2 + \left(\Psi_y + \beta \frac{\partial W}{\partial y} \right)^2 \right] + \lambda_x \left(\frac{\partial W}{\partial x} \right)^2 + \beta^4 \lambda_y \left(\frac{\partial W}{\partial y} \right)^2 \right\} dx dy. \tag{26}$$

The maximum kinetic energy for free harmonic vibration is

$$T = \frac{1}{2} \omega^2 \int_{-\pi/2}^{\pi/2} \int_{-\pi/2}^{\pi/2} (\theta^2 W^2 + \Psi_x^2 + \Psi_y^2) dx dy \tag{27}$$

and the strain energy owing to the Pasternak foundation model is

$$V = \frac{1}{2} \int_{-\pi/2}^{\pi/2} \int_{-\pi/2}^{\pi/2} \left\{ K_1 W^2 + K_2 \left[\left(\frac{\partial W}{\partial x} \right)^2 + \beta^2 \left(\frac{\partial W}{\partial y} \right)^2 \right] \right\} dx dy \tag{28}$$

then the energy functional is

$$\Pi = U - T + V. \tag{29}$$

3.2. ADMISSIBLE SOLUTION

Firstly, we assume the modal shape functions as

$$W(x, y) = W_I + W_{II} + W_{III} + W_{IV}, \tag{30}$$

$$\Psi_x(x, y) = \Psi_{xII} + \Psi_{xIV}, \tag{31}$$

$$\Psi_y(x, y) = \Psi_{yIII} + \Psi_{yIV}, \tag{32}$$

where

$$W_I = A_{00}, \quad W_{II} = \sum_{m=1,2,\dots} [A_{m0} \cos(2mx) + a_{1m0} x^2], \tag{33a, 33b}$$

$$W_{III} = \sum_{n=1,2,\dots} [A_{0n} \cos(2ny) + a_{20n} y^2], \tag{33c}$$

$$W_{IV} = \sum_{n=1,2,\dots} [A_{1mn} \cos(2mx) + A_{2mn} \cos(2ny) + A_{mn} \cos(2mx) \cos(2ny) + a_{1mn}x^2 + a_{2mn}y^2], \tag{33d}$$

$$\Psi_{xII} = \sum_{m=1,2,\dots} [B_{m0} \sin(2mx) + b_{1m0}x], \tag{33e}$$

$$\Psi_{xIV} = \sum_{m=1,2,\dots} [B_{1mn} \sin(2mx) + B_{mn} \sin(2mx) \cos(2ny) + b_{1mn}x], \tag{33f}$$

$$\Psi_{yIII} = \sum_{n=1,2,\dots} [C_{0n} \sin(2ny) + c_{20n}y], \tag{33g}$$

$$\Psi_{yIV} = \sum_{n=1,2,\dots} [C_{2mn} \sin(2ny) + C_{mn} \cos(2mx) \sin(2ny) + c_{2mn}y] \tag{33h}$$

in which, A_{00} , A_{m0} , etc. are unknown coefficients. Because the applied loads in section 4 are symmetric, only the double symmetric modals will make contributions to the dynamic response of the plate. For this reason, the modal shape functions selected here are applicable to cases of double symmetry.

Then substituting equations (30)–(32) into equations (16) and (17), considering the boundary conditions (24) and ignoring the thermal bending and the dynamic inertia, we can set-up the relations among the unknown coefficients. They are

$$\begin{bmatrix} W_{II} \\ \Psi_{xII} \end{bmatrix} = \begin{bmatrix} \mathbf{w}_2^* \\ \Psi_{x2}^* \end{bmatrix} \mathbf{a}_2^T, \tag{34a}$$

$$\begin{bmatrix} W_{III} \\ \Psi_{yIII} \end{bmatrix} = \begin{bmatrix} \mathbf{w}_3^* \\ \Psi_{y3}^* \end{bmatrix} \mathbf{a}_3^T, \tag{34b}$$

$$\begin{bmatrix} W_{IV} \\ \Psi_{xIV} \\ \Psi_{yIV} \end{bmatrix} = \begin{bmatrix} \mathbf{w}_4^* \\ \Psi_{x4}^* \\ \Psi_{y4}^* \end{bmatrix} \mathbf{a}_4^T, \tag{34c}$$

in which the row-submatrix of \mathbf{w}_2^* , Ψ_{x2}^* , etc., are defined in Appendix A.

Using the Rayleigh–Ritz method and minimizing the total energy functional of equation (29) with respect to the unknown coefficients leads to

$$(\mathbf{D} + \lambda_x \mathbf{E} - \omega^2 \mathbf{F}) \mathbf{a} = 0, \tag{35}$$

where \mathbf{a} is the column matrix of all unknown coefficients (generalized displacements), \mathbf{D} is the elastic stiffness matrix, \mathbf{E} the initial stress stiffness matrix and \mathbf{F} the consistent mass matrix. The details of these matrices are given in Appendix B. If the truncated orders of the admissible functions $m = n = r - 1$, the size of these matrices is $r^2 \times r^2$. Because not all of the elements of \mathbf{a} equal to zero, from equation (35), we have

$$\det(\mathbf{D} + \lambda_x \mathbf{E} - \omega^2 \mathbf{F}) = 0. \tag{36}$$

The resultant standard eigenequation can then be easily solved for determining the m order natural frequencies ω_m and mode shape functions $W_m(x, y)$, $\Psi_{xm}(x, y)$ and $\Psi_{ym}(x, y)$, which satisfy both geometrical and natural boundary conditions, and will be used in the next section for dynamic analysis.

4. FORCED VIBRATION ANALYSIS

Because the boundary condition of equation (24) is non-homogeneous, we assume that the solution of equations (15)–(17) is comprised of two parts as [17, 18]

$$W(x, y, t) = \tilde{W}(x, y, t) + \hat{W}(x, y), \quad (37a)$$

$$\Psi_x(x, y, t) = \tilde{\Psi}_x(x, y, t) + \hat{\Psi}_x(x, y), \quad (37b)$$

$$\Psi_y(x, y, t) = \tilde{\Psi}_y(x, y, t) + \hat{\Psi}_y(x, y), \quad (37c)$$

where $\hat{W}(x, y)$, $\hat{\Psi}_x(x, y)$ and $\hat{\Psi}_y(x, y)$ are additional solutions, and assumed to have the form

$$\hat{W}(x, y) = M^T[\alpha_{11} \cos(2x) + \alpha_{12} \cos(2y) + \alpha_{13} \cos(2x) \cos(2y) + \alpha_{14} x^2 + \alpha_{15} y^2], \quad (38a)$$

$$\hat{\Psi}_x(x, y) = M^T[\alpha_{21} \sin(2x) + \alpha_{23} \sin(2x) \cos(2y) + \alpha_{24} x], \quad (38b)$$

$$\hat{\Psi}_y(x, y) = M^T[\alpha_{32} \sin(2y) + \alpha_{33} \cos(2x) \sin(2y) + \alpha_{35} y]. \quad (38c)$$

Substituting solution (38) into equations (15)–(17) and boundary condition (24), the coefficients α_{11} , α_{12} , etc. can be determined with details given in Appendix C.

Then solutions $\tilde{W}(x, y)$, $\tilde{\Psi}_x(x, y)$ and $\tilde{\Psi}_y(x, y)$ should satisfy equations

$$L_{11}(\tilde{\Psi}_x) + L_{12}(\tilde{\Psi}_y) + L_{13}(\tilde{W}) - K_1 \tilde{W} + K_2 \bar{\nabla}^2 \tilde{W} + \tilde{\lambda}_q = L_{14}(\tilde{W}), \quad (39a)$$

$$L_{21}(\tilde{\Psi}_x) + L_{22}(\tilde{\Psi}_y) + L_{23}(\tilde{W}) = L_{24}(\tilde{\Psi}_x), \quad (39b)$$

$$L_{31}(\tilde{\Psi}_x) + L_{32}(\tilde{\Psi}_y) + L_{33}(\tilde{W}) = L_{34}(\tilde{\Psi}_y) \quad (39c)$$

with the homogeneous boundary conditions

$$x = \mp \pi/2:$$

$$\frac{\partial \tilde{\Psi}_x}{\partial x} + \nu \beta \frac{\partial \tilde{\Psi}_y}{\partial y} = 0, \quad \beta \frac{\partial \tilde{\Psi}_x}{\partial y} + \frac{\partial \tilde{\Psi}_y}{\partial x} = 0, \quad \frac{\partial \tilde{W}}{\partial x} + \tilde{\Psi}_x = 0. \quad (40a)$$

$$y = \mp \pi/2:$$

$$\nu \frac{\partial \tilde{\Psi}_x}{\partial x} + \beta \frac{\partial \tilde{\Psi}_y}{\partial y} = 0, \quad \beta \frac{\partial \tilde{\Psi}_x}{\partial y} + \frac{\partial \tilde{\Psi}_y}{\partial x} = 0, \quad \beta \frac{\partial \tilde{W}}{\partial y} + \tilde{\Psi}_y = 0 \quad (40b)$$

and the initial condition

$$(\tilde{W}, \tilde{\Psi}_x, \tilde{\Psi}_y)|_{t=0} = -(\hat{W}, \hat{\Psi}_x, \hat{\Psi}_y) \left(\frac{\partial \tilde{W}}{\partial t}, \frac{\partial \tilde{\Psi}_x}{\partial t}, \frac{\partial \tilde{\Psi}_y}{\partial t} \right) \Big|_{t=0} = - \left(\frac{\partial \hat{W}}{\partial t}, \frac{\partial \hat{\Psi}_x}{\partial t}, \frac{\partial \hat{\Psi}_y}{\partial t} \right) = 0 \quad (41)$$

in equation (39a) $\tilde{\lambda}_q$ is given in detail in Appendix D.

The modal superposition approach (MSA) is now used to solve equation (39) and we assume

$$\tilde{W}(x, y, t) = \sum_{m=1}^{\infty} W_m(x, y) T_m(t), \quad (42a)$$

$$\tilde{\Psi}_x(x, y, t) = \sum_{m=1}^{\infty} \Psi_{xm}(x, y) T_m(t), \tag{42b}$$

$$\tilde{\Psi}_y(x, y, t) = \sum_{m=1}^{\infty} \Psi_{ym}(x, y) T_m(t), \tag{42c}$$

where $W_m(x, y)$, $\Psi_{xm}(x, y)$ and $\Psi_{ym}(x, y)$ come from equation (35) and $T_m(t)$ is the principal co-ordinate for the m th modal and ω_m is the m th frequency of the plate. Following the same procedure of reference [1], we can obtain

$$T_m(t) = \frac{I_m}{K_m} \cos(\omega_m t) + \frac{1}{\omega_m K_m} \int_0^t Q_m(\tau) \sin[\omega_m(t - \tau)] d\tau, \tag{43}$$

where $Q_m(t)$, K_m , I_m are given in detail in Appendix D. Note that the Mindlin–Goodman orthogonality condition, in the present case, can be written as

$$\int_0^\pi \int_0^\pi [\theta^2 W_m(x, y) W_n(x, y) + \Psi_{xm}(x, y) \Psi_{xn}(x, y) + \Psi_{ym}(x, y) \Psi_{yn}(x, y)] dx dy$$

$$= 0 \quad \text{when } m \neq n$$

$$\neq 0 \quad \text{when } m = n \quad (m, n = 1, 2, 3, \dots). \tag{44}$$

Substituting equation (43) into equation (42) and adding equation (38), $W(x, y, t)$, $\Psi_x(x, y, t)$ and $\Psi_y(x, y, t)$ can be obtained. If we degenerate this problem into a static one, $T_m(t)$, $Q_m(t)$ become independent on time, then we can seek the static solution. Taking the same procedure as its dynamic counterpart, we can obtain

$$T_m = \frac{Q_m}{K_m(\omega_m)^2}. \tag{45}$$

Using the same steps, the displacement fields can be expressed explicitly.

5. NUMERICAL EXAMPLES AND COMMENTS

5.1. CONVERGENCE AND COMPARISON STUDIES

To demonstrate the convergence of the presented method, a study of free or forced vibration for a square plate with four free edges has been carried out by setting $\nu = 0.15$, $\kappa^2 = \pi^2/12$ and $\rho = 2500 \text{ kg/m}^3$. The plate is supported by a Pasternak-type elastic foundation with $(k_1, k_2) = (2.0, 0.4)$, but no edge compression is applied. For free vibration problem, no thermal bending stress is included, and the symmetric–symmetric (SS) dimensionless frequency $\bar{\omega} = \Omega b^2/\pi^2 \sqrt{\rho h/D}$ is given in Table 1 for various width-to-thickness ratio $b/h = 5, 10$ and 20 . It is mentioned that the first frequencies in Table 1 are the rigid-body translations on elastic foundations. The results indicate that the first five SS frequencies converge very accurately by taking m and n up to 5. Accordingly, in the following studies, m and n are taken as 5. For a dynamic problem, initial thermal bending stress is included ($T_0 = 30^\circ\text{C}$, $\alpha = 1.0 \times 10^{-5}/^\circ\text{C}$, $C = 1.0$), dimensionless dynamic deflection ($\hat{W} = \bar{W}Eah/q_0b^3$) and bending moment ($\hat{M}_x = \bar{M}_xa^2/q_0b^2h^2$) as function of time [$\hat{t} = (\bar{t}/b) \sqrt{E/\rho}$] are listed in Table 2 for a square plate with $b/h = 10$ subjected to

TABLE 1

Convergence study for the symmetric-symmetric frequency parameter $\Omega b^2/\pi^2 \sqrt{\rho h/D}$ of square plates; $\nu = 0.15$, $a/b = 1$, and $(k_1, k_2) = (2.0, 0.4)$

		Determinant size	Doubly symmetric modes				
<i>m</i>	<i>n</i>		1	2	3	4	5
<i>b/h = 5</i>	1	4	1.4142	2.7038	2.8753	6.5002	—
	3	16	1.4142	2.6739	2.8099	5.5620	8.6598
	4	25		2.6683	2.8063	5.6470	8.3287
	5	36		2.6678	2.8059	5.6453	8.3156
	6	49		2.6678	2.8059	5.6451	8.3146
<i>b/h = 10</i>	1	4	1.4142	2.8830	3.0799	7.5266	—
	3	16	1.4142	2.8556	3.0104	6.6793	11.0073
	4	25		2.8535	3.0088	6.6680	10.7577
	5	36		2.8533	3.0086	6.6673	10.7476
	6	49		2.8533	3.0086	6.6673	10.7468
<i>b/h = 20</i>	1	4	1.4142	2.9382	3.1440	7.8917	—
	3	16	1.4142	2.9128	3.0743	7.0793	12.1290
	4	25		2.9117	3.0734	7.0684	11.9587
	5	36		2.9116	3.0733	7.0678	11.9529
	6	49		2.9116	3.0733	7.0678	11.9526

a suddenly applied central patch load ($a_1/a = b_1/b = 0.5$, $q_0 = 2.0 \times 10^3$ kN/m², $E = 35$ GN/m²). The results indicate that the convergence is obtained by taking numbers of modes up to 14, which is employed in the following dynamic studies.

As part of the validation of the present method, the central deflections and bending stress of a free edge moderately thick square plate, subjected to a static transverse load over a central patch area alone and resting on a Winkler elastic foundation, are compared in Figure 2 with finite-difference method results given by Henwood *et al.* [22] and the superposition method solutions given by Shi *et al.* [23], using their computing data, i.e., $E = 300$ MN/m², $\nu = 0.35$, $\bar{K}_1 = 50$ MN/m², $a = b = 1.0$ m, $h = 0.4$ m, $a_1 = b_1 = 0.5$ m, and $q_0 = 1.0$ N/m². They show that, in the static bending case, the deflection \bar{W} along the X -axis is in good agreement with the comparison results, whereas the bending stress $\bar{\sigma}_x$ along the X -axis is lower than its counterparts, when $0.2 < X < 0.8$ m.

In addition, the dimensionless frequencies for completely free square and rectangular thick plates (that means without any elastic foundation) are compared in Table 3 with Rayleigh-Ritz solutions of Frederiksen [11] (taking orthogonal polynomials as admissible functions) and Hanna [2] (taking polynomials as admissible functions) and superposition method solution of Gorman [14]. Rigid-body translations are not included. They show that, in the free vibration case, the present results agree well with existing solutions.

5.2. PARAMETRIC STUDIES

A parametric study intended to supply information on the dynamic behaviors of a moderately thick plate with four free edges subjected to thermomechanical loading and resting on an elastic foundation was undertaken. The typical results are shown in Figures 3-9. It should be appreciated that in all these figures $(\bar{t}/b)\sqrt{E/\rho}$, $\bar{W}Eah/q_0b^3$, $\bar{M}_x a^2/q_0b^2h^2$ mean

TABLE 2

Convergence study for the dimensionless dynamic deflection ($\hat{W} = \bar{W}Eah/q_0b^3$) and dynamic bending ($\hat{M}_X = \bar{M}_Xa^2/q_0b^2h^2$) moment of square plates; $\nu = 0.15$, $a/b = 1$, $b/h = 10$, $(k_1, k_2) = (2.0, 0.4)$, $a_1/a = b_1/b = 0.5$, $q_0 = 2.0 \times 10^3$ kN/m², $T_0 = 30^\circ\text{C}$, $\alpha = 1.0 \times 10^{-5}/^\circ\text{C}$, $C = 1.0$

No. of modes	$\hat{t} = 2$		$\hat{t} = 4$		$\hat{t} = 6$		$\hat{t} = 8$		$\hat{t} = 10$		$\hat{t} = 12$	
	\hat{W}	\hat{M}_X	\hat{W}	\hat{M}_X	\hat{W}	\hat{M}_X	\hat{W}	\hat{M}_X	\hat{W}	\hat{M}_X	\hat{W}	\hat{M}_X
6	2.1421	2.8246	3.9263	3.6340	3.6050	1.6101	3.7712	1.5715	4.4510	3.1225	3.2592	3.2836
8	2.1502	2.8733	3.9340	3.6801	3.6071	1.6228	3.7797	1.6223	4.4582	3.1658	3.2614	3.2970
10	2.1467	2.8430	3.9307	3.6520	3.6042	1.5982	3.7773	1.6022	4.4565	3.1509	3.2603	3.2878
12	2.1337	2.7315	3.9202	3.5620	3.5974	1.5395	3.7746	1.5784	4.4574	3.1590	3.2639	3.3185
14	2.1269	2.6674	3.9136	3.4996	3.5971	1.5358	3.7676	1.5127	4.4509	3.0983	3.2635	3.3147
16	2.1271	2.6725	3.9140	3.5042	3.5973	1.5376	3.7678	1.5156	4.4511	3.1000	3.2635	3.3152

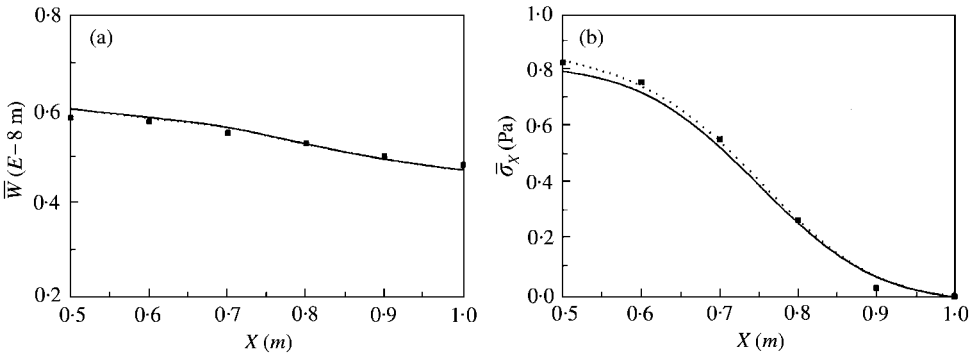


Figure 2. The comparison of static deflection and flexural stress along the X direction: (a) deflection; (b) flexural stress: —, present; ■, Henwood et al. (1982); ·····, Shi et al. (1994).

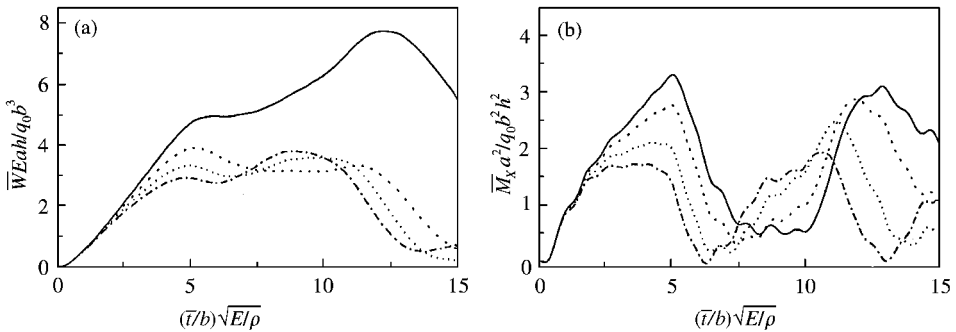


Figure 3. Effect of the foundation stiffness on dynamic behaviors of a moderately thick plate: (a) central deflection versus time; (b) bending moment versus time ($\beta = 1.0$, $b/h = 10.0$, $N_x = 0$, $a_1/a = b_1/b = 0.5$): —, $(k_1, k_2) = (1.0, 0.0)$; - - - - -, $(k_1, k_2) = (2.0, 0.0)$; ·····, $(k_1, k_2) = (2.0, 0.4)$; - · - · - ·, $(k_1, k_2) = (2.0, 0.8)$.

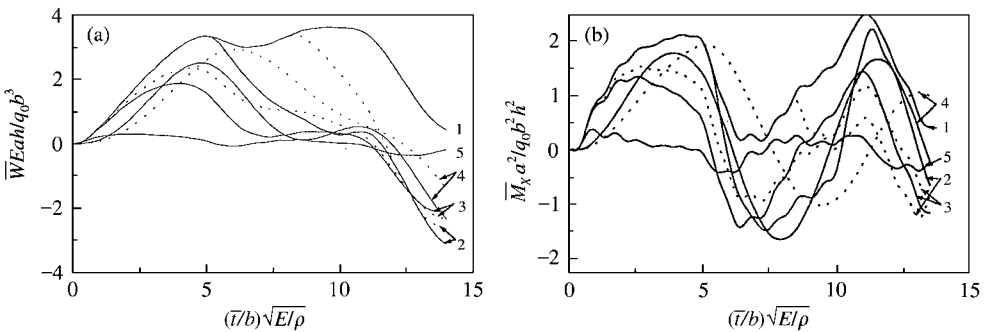


Figure 4. Effect of pulse shape and pulse duration on dynamic behaviors of a moderately thick plate: (a) central deflection versus time; (b) bending moment versus time ($\beta = 1.0$, $b/h = 10.0$, $(k_1, k_2) = (2.0, 0.4)$, $N_x = 0$, $a_1/a = b_1/b = 0.5$): 1, Load Case 1; 2, Load Case 2; 3, Load Case 3; 4, Load Case 4; 5, Load Case 5. —, $(\bar{t}_0/b) \sqrt{E/\rho} = 5.0$; ·····, $(\bar{t}_0/b) \sqrt{E/\rho} = 8.0$.

the dimensionless forms of, respectively, time, central deflection and bending moment of the plate, i.e., at the point $(X, Y) = (0, 0)$. For all of the examples, $E = 35 \text{ GN/m}^2$, $\nu = 0.15$, $\rho = 2500 \text{ kg/m}^3$, and the transverse shear correction factor was considered to be $\kappa^2 = \pi^2/12$. The impulsive pressure $q(X, Y, \bar{t}) = q_0 F(\bar{t}) f(X, Y)$ is applied on the top surface

TABLE 3
Comparisons of frequencies of completely free plates

Dimensionless forms	b/h	a/b	Doubly symmetric modes						
			SS-1	SS-2	SS-3				
$\Omega a^2 \sqrt{\rho/E}/h$	$\nu = 0.3$ $\kappa^2 = \pi^2/12$	6.67	Frederiksen [11]	FEM	6.2515	13.998	30.636		
				FSDPT	6.2513	13.997	30.632		
				HSDPT	6.2473	13.976	30.499		
		10	Hanna [2]	Present	1.5	FSDPT	6.2515	13.9879	30.5603
				1	FSDPT	5.732	7.057	16.845	
				2	HSDPT	5.736	7.065	16.896	
$\Omega a^2 \sqrt{\rho/E}/h$	$\nu = 0.15$ $\kappa^2 = \pi^2/12$	10	Gorman [14]	FSDPT	6.430	25.665	34.012		
				HSDPT	6.432	25.691	34.073		
				Present	1	FSDPT	5.7355	7.0673	16.9213
		10	Present	2	FSDPT	6.4350	25.6866	34.0863	
				1	SM	18.59	23.45	54.90	
				0.5		5.257	21.10	27.93	
$\Omega a^2 \sqrt{\rho h/D}$	$\nu = 0.333$ $\kappa^2 = 0.8601$	10	Present	1	RRM	18.5996	23.4966	55.4550	
				0.5		5.2623	21.1271	28.1052	

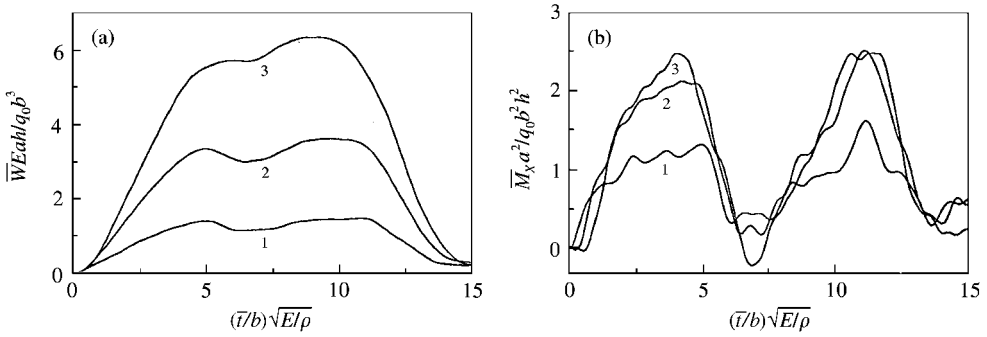


Figure 5. Effect of loaded area on dynamic behaviors of a moderately thick plate: (a) central deflection versus time; (b) bending moment versus time ($\beta = 1.0$, $b/h = 10.0$, $(k_1, k_2) = (2.0, 0.4)$, $N_X = 0$): 1, $a_1/a = b_1/b = 0.3$; 2, $a_1/a = b_1/b = 0.5$; 3, $a_1/a = b_1/b = 0.7$.

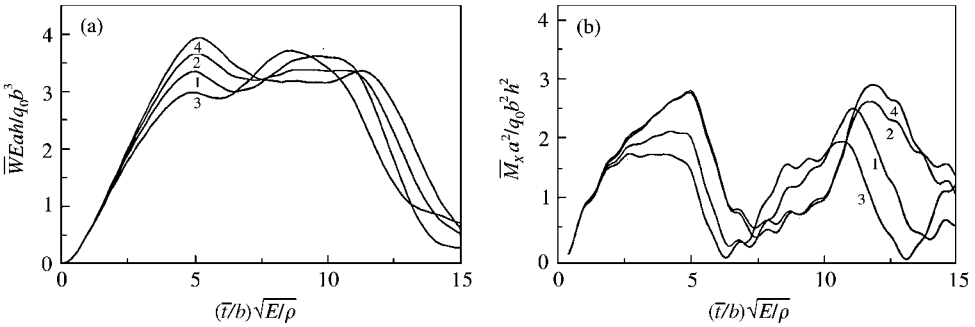


Figure 6. Effect of initial membrane stress on dynamic behaviors of a moderately thick plate: (a) central deflection versus time; (b) bending moment versus time ($\beta = 1.0$, $b/h = 10.0$, $(k_1, k_2) = (2.0, 0.4)$, $a_1/a = b_1/b = 0.5$): 1, $\chi = 0.0$, $N_X/(N_X)_{cr} = 0.0$; 2, $\chi = 0.0$, $N_X/(N_X)_{cr} = -0.25$; 3, $\chi = 0.0$, $N_X/(N_X)_{cr} = 0.25$; 4, $\chi = 1.0$, $N_X/(N_X)_{cr} = -0.25$.

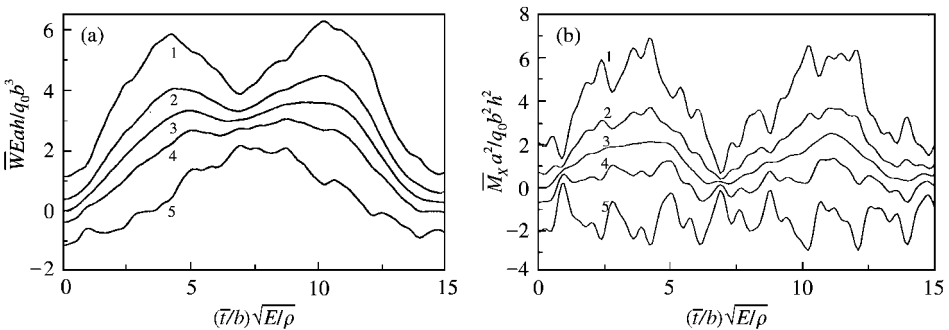


Figure 7. Effect of the initial thermal bending stress on dynamic behaviors of a moderately thick plate: (a) central deflection versus time; (b) bending moment versus time ($\beta = 1.0$, $b/h = 10.0$, $T_0 = 30^\circ\text{C}$, $(k_1, k_2) = (2.0, 0.4)$, $N_X = 0$, $a_1/a = b_1/b = 0.5$): 1, $C = 3.0$; 2, $C = 1.0$; 3, $C = 0.0$; 4, $C = -1.0$; 5, $C = -3.0$.

of the plate, in which q_0 is the maximum amplitude, $f(X, Y)$ is a unit function in space domain and $F(\bar{t})$ is a unit function in time domain which can be any one of the types listed in Table 4.

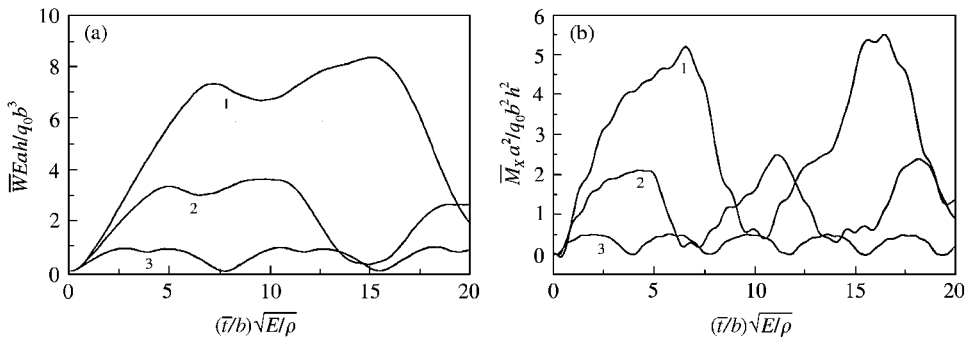


Figure 8. Effect of the plate width-to-thickness ratio on dynamic behaviors of a moderately thick plate: (a) central deflection versus time; (b) bending moment versus time ($\beta = 1.0$, $(k_1, k_2) = (2.0, 0.4)$, $N_x = 0$, $a_1/a = b_1/b = 0.5$); 1, $b/h = 15.0$; 2, $b/h = 10.0$; 3, $b/h = 5.0$.

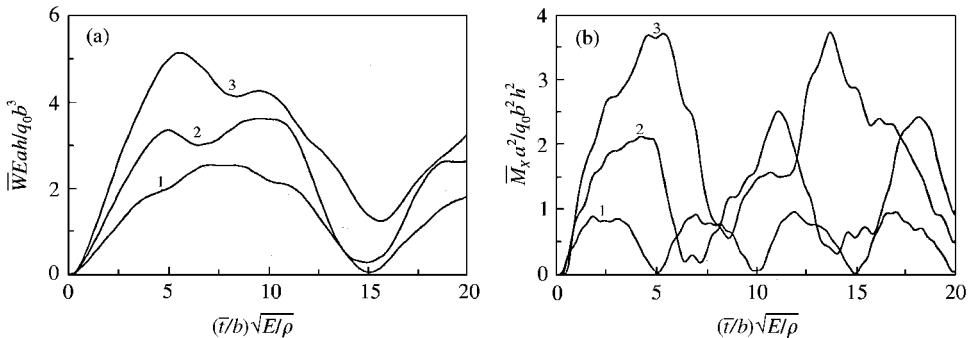


Figure 9. Effect of the plate aspect ratio on dynamic behaviors of a moderately thick plate: (a) central deflection versus time; (b) bending moment versus time ($b/h = 10.0$, $(k_1, k_2) = (2.0, 0.4)$, $N_x = 0$, $a_1/a = b_1/b = 0.5$); 1, $\beta = 0.75$; 2, $\beta = 1.00$; 3, $\beta = 1.25$.

Figure 3 shows central deflection and bending moment as functions of time for a square plate subjected to a suddenly applied central patch load and either resting on Pasternak-type or Winkler elastic foundations. The stiffnesses are $(k_1, k_2) = (2.0, 0.8)$ and $(k_1, k_2) = (2.0, 0.4)$ for Pasternak-type elastic foundations and $(k_1, k_2) = (2.0, 0.0)$ and $(k_1, k_2) = (1.0, 0.0)$ for Winkler elastic foundations. It can be seen that the foundation stiffness has a significant effect on the dynamic response of the plate.

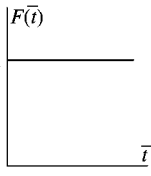
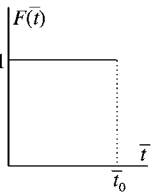
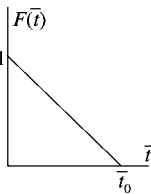
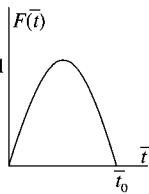
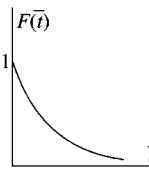
Figure 4 shows the effect of the pulse shape and duration on the dynamic response of a thick square plate under the loading condition of cases 1–5, i.e., sudden loads, step loads, triangular loads, sine loads and exponential loads in Table 4, when the plate is supported by a Pasternak-type elastic foundation. Here $(\bar{t}_0/b)\sqrt{E/\rho} = 5.0$ and 8.0 indicates pulse duration.

Figure 5 shows the effect of the loaded area parameter ($a_1/a = b_1/b = 0.3, 0.5$, and 0.7) on the dynamic response of a thick square plate subjected to a suddenly applied load and resting on a Pasternak-type elastic foundation. As expected, these results show that the central deflections and bending moments are decreased by decreasing the loaded area parameter.

Figure 6 shows the effect of initial membrane stress (compressive or tensile) on the dynamic response of a thick square plate subjected to a suddenly applied central patch load

TABLE 4

The various kinds of pulse shapes of transverse impulsive loads

Case	1	2	3	4	5
	Sudden loads	Step loads	Triangular loads	Sine loads	Exponential loads
					
	$F(\bar{t}) = 1$	$F(\bar{t}) = \begin{cases} 1, & \bar{t} \leq \bar{t}_0 \\ 0, & \bar{t} > \bar{t}_0 \end{cases}$	$F(\bar{t}) = \begin{cases} 1 - \frac{\bar{t}}{\bar{t}_0}, & \bar{t} \leq \bar{t}_0 \\ 0, & \bar{t} > \bar{t}_0 \end{cases}$	$F(\bar{t}) = \begin{cases} \sin \frac{\pi \bar{t}}{\bar{t}_0}, & \bar{t} \leq \bar{t}_0 \\ 0, & \bar{t} > \bar{t}_0 \end{cases}$	$F(\bar{t}) = e^{-\alpha \bar{t}}$

and resting on a Pasternak-type elastic foundation. Clearly, the in-plane loads have considerable effects on the dynamic behavior of the plate, but the biaxial load ratio has less effect.

Figure 7 shows the effect of initial thermal bending stress ($q_0 = 2.0 \times 10^3$ kN/m², $E = 35$ GN/m², $T_0 = 30^\circ\text{C}$, $\alpha = 1.0 \times 10^{-5}/^\circ\text{C}$, $C = 0.0, \pm 1.0$ and ± 3.0) on the dynamic response of a thick square plate subjected to a suddenly applied central patch load and resting on a Pasternak-type elastic foundation.

Numerical values for some points on the curves analogous to the results of Figures 6 and 7 are listed in Table 5. These numerical results are useful for numerical benchmarking by others.

Figures 8 and 9 show, respectively, plate width-to-thickness ratio b/h ($= 15.0, 10.0$ and 5.0) and plate aspect ratio β ($= 0.75, 1.0$ and 1.25) on the dynamic response of a rectangular plate subjected to a suddenly applied central patch load and resting on a Pasternak-type elastic foundation. It can be seen that the transverse shear deformation has a significant effect on the dynamic behavior. Also, it can be seen that the central deflections and bending moments are increased, but the frequency is decreased by increasing the plate aspect ratio.

In Figures 4–9, the Pasternak-type elastic foundation stiffness is characterized by $(k_1, k_2) = (2.0, 0.4)$; in Figures 3 and 5–9, the plate is subjected to a suddenly applied central patch load; in Figures 3 and 4 and 6–9, the loaded area parameter $a_1/a = b_1/b = 0.5$; in Figures 3–5 and 7–9, biaxial load ratio $\chi = 0.0$ and the initial compressive stress $N_x = 0$; in Figures 3–6 and 8 and 9, the temperature gradient $C = 0.0$; in Figures 3–7 and 9, the plate width-to-thickness ratio $b/h = 10.0$; and in Figures 3–8, the plate aspect ratio $\beta = 1.0$.

6. CONCLUSIONS

Free and forced vibration analysis for a Reissner–Mindlin plate with four free edges resting on a Pasternak-type elastic foundation has been presented. A new set of admissible functions, which satisfy both geometrical and natural boundary conditions, is developed for the free vibration analysis of moderately thick plates with four free edges. On this basis, the modal superposition approach is used in conjunction with Mindlin–Goodman procedure

TABLE 5

The dimensionless dynamic deflection ($\hat{W} = \bar{W}Eah/q_0b^3$) and dynamic bending moment ($\hat{M}_X = \bar{M}_Xa^2/q_0b^2h^2$) at different times ($\hat{t} = (\bar{t}/b)\sqrt{E/\rho}$) of square plates; $\nu = 0.15$, $a/b = 1$, $b/h = 10$, $(k_1, k_2) = (2.0, 0.4)$, $a_1/a = b_1/b = 0.5$, $q_0 = 2.0 \times 10^3 \text{ kN/m}^2$, $T_0 = 30^\circ\text{C}$, $\alpha = 1.0 \times 10^{-5}/^\circ\text{C}$

Initially stressed	\hat{t}	2	4	6	8	10	12	14
$N_X/(N_X)_{cr} = 0$	\hat{W}	1.4266	3.0003	3.0633	3.3105	3.5822	2.4291	0.4055
	\hat{M}_X	1.5781	2.0846	0.6180	0.6529	1.6199	1.8385	0.3109
$N_X/(N_X)_{cr} = -0.25$	\hat{W}	1.4550	3.1921	3.4012	3.2578	3.3371	2.7614	0.8796
	\hat{M}_X	1.6323	2.5165	1.4949	0.6080	0.9750	2.5918	1.6374
$N_X/(N_X)_{cr} = 0.25$	\hat{W}	1.3987	2.8474	2.9084	3.4745	3.5680	1.9965	0.5343
	\hat{M}_X	1.5189	1.7268	0.1840	1.0397	1.6944	0.7610	0.5410
$N_X/(N_X)_{cr} = N_Y/(N_X)_{cr} = 0.25$	\hat{W}	1.4804	3.3553	3.6740	3.1620	3.1408	3.1248	1.3001
	\hat{M}_X	1.6662	2.5204	1.5447	0.4512	1.0103	2.9099	1.5053
Initially heated	\hat{t}	2	4	6	8	10	12	14
$C = 1.0$	\hat{W}	2.1274	3.9140	3.5974	3.7678	4.4511	3.2635	0.8406
	\hat{M}_X	2.6725	3.5042	1.5397	1.5157	3.1001	3.3152	1.2267
$C = -1.0$	\hat{W}	0.7259	2.0865	2.5292	2.8531	2.7133	1.5946	-0.0296
	\hat{M}_X	0.4837	0.6650	-0.3038	-0.2098	0.1396	0.3617	-0.6049

to determine the dynamic response of free edge Reissner-Mindlin plates exposed to thermomechanical loading. The static bending problem is treated as a limiting case. A number of issues related to static bending and free vibration of free edge moderately thick plates with or without elastic foundations have been examined.

Some numerical results are given for the first time and can serve as a benchmark for further investigations. A parametric study of free edge moderately thick plates resting on Winkler or Pasternak-type elastic foundations has been carried out. The results presented herein confirm that the characteristics of dynamic behavior are significantly influenced by foundation stiffness, shape and duration of impulsive load, loaded area, transverse shear deformation, plate aspect ratio as well as initial membrane stress.

REFERENCES

1. H. S. SHEN, J. YANG and L. ZHANG 2000 *Journal of Sound and Vibration* **232**, 309-329. Dynamic response of Reissner-Mindlin plates under thermomechanical loading and resting on elastic foundations.
2. N. F. HANNA and A. W. LEISSA 1994 *Journal of Sound and Vibration* **170**, 545-555. A higher order shear deformation theory for the vibration of thick plates.
3. R. JONES and B. J. MILNE 1976 *Journal of Sound and Vibration* **45**, 309-316. Application of the extended Kantorovich method to the vibration of clamped rectangular plates.
4. R. B. BHAT, J. SINGH and G. MUNDKAR 1993 *Journal of Vibration and Acoustics, American Society of Mechanical Engineers* **115**, 177-181. Plate characteristic functions and natural frequencies of vibration of plates by iterative reduction of partial differential equation.
5. C. RAJALINGHAM, R. B. BHAT and G. D. XISTRIS 1996 *Journal of Sound and Vibration* **197**, 263-281. Closed form approximation of vibration modes of rectangular cantilever plates by the variational reduction method.
6. W. RITZ 1909 *Annalen der Physik, Viente Folge* **28**, 737-786. Theorie der transversalschwingungen einer quadratischen platten mit freien randem.

7. S. F. BASSILY and S. M. DICKINSON 1975 *Journal of Applied Mechanics* **42**, 858–864. On the use of beam functions for problems of plates involving free edges.
8. D. J. DAWE and O. L. ROUFAEIL 1980 *Journal of Sound and Vibration* **69**, 345–359. Rayleigh–Ritz vibration analysis of Mindlin plates.
9. S. F. BASSILY and S. M. DICKINSON 1978 *Journal of Sound and Vibration* **59**, 1–14. Buckling and vibration of in-plane loaded plates treated by a unified Ritz approach.
10. S. M. DICKINSON and D. A. BLASIO 1986 *Journal of Sound and Vibration* **108**, 51–62. On the use of orthogonal polynomials in the Rayleigh–Ritz method for the study of the flexural vibration and buckling of isotropic and orthotropic rectangular plates.
11. P. S. FREDERIKSEN 1995 *Journal of Sound and Vibration* **186**, 743–759. Single-layer plate theories applied to the flexural vibration of completely free thick laminates.
12. K. M. LIEW, Y. XIANG and S. KITIPORNCHAI 1993 *Computers and Structures* **49**, 1–29. Transverse vibration of thick rectangular plates-I, comprehensive sets of boundary conditions.
13. D. J. GORMAN 1993 *Journal of Sound and Vibration* **165**, 409–420. Accurate free vibration analysis of the completely free orthotropic rectangular plate by the method of superposition.
14. D. J. GORMAN and W. DING 1993 *Journal of Sound and Vibration* **189**, 341–353. Accurate free vibration analysis of the completely free rectangular Mindlin plate.
15. H. S. SHEN 1998 *American Society of Civil Engineers Journal of Engineering Mechanics* **124**, 1080–1089. Large deflection of Reissner–Mindlin plates on elastic foundations.
16. H. S. SHEN 1999 *International Journal of Mechanical Sciences* **41**, 845–864. Nonlinear bending of Reissner–Mindlin plates with free edges under transverse and in-plane loads and resting on elastic foundations.
17. R. D. MINDLIN and L. E. GOODMAN 1950 *Journal of Applied Mechanics* **17**, 377–380. Beam vibrations with time-dependent boundary conditions.
18. C. T. SUN and J. M. WHITNEY 1974 *Journal of Acoustic Society in America* **55**, 1003–1008. Forced vibration of laminated composite plates in cylindrical bending.
19. Y. XIANG, C. M. WANG and S. KITIPORNCHAI 1994 *International Journal of Mechanical Sciences* **36**, 311–316. Exact vibration solution for initially stressed Mindlin plates on Pasternak foundations.
20. L. LIBRESCU and W. LIN 1997 *International Journal of Non-linear Mechanics* **32**, 211–225. Postbuckling and vibration of shear deformable flat and curved panels on a non-linear elastic foundation.
21. H. S. SHEN 1996 *Structural Engineering and Mechanics* **4**, 149–162. Thermomechanical postbuckling of imperfect moderate thick plates on two-parameter elastic foundations.
22. D. J. HENWOOD, J. WHITEMAN and A. L. YETTRAM 1982 *International Journal for Numerical Methods in Engineering* **18**, 1801–1820. Fourier series solution for a rectangular thick plate with free edges on a elastic foundation.
23. X. P. SHI, S. A. TAN and T. F. FWA 1994 *American Society of Civil Engineers Journal of Engineering Mechanics*, **120**, 971–988. Rectangular thick plate with free edges on Pasternak foundation.

APPENDIX A

In equation (34),

$$\begin{aligned}
 \mathbf{a}_1 &= [A_{00}], \quad \mathbf{a}_2 = [A_{10} \cdots A_{m0}], \quad \mathbf{a}_3 = [A_{01} \cdots A_{0n}], \quad \mathbf{a}_4 = [A_{11} \cdots A_{mn}], \\
 \mathbf{w}_1^* &= [1], \quad \mathbf{w}_2^* = [w_{10} \cdots w_{m0}], \quad \mathbf{w}_3^* = [w_{01} \cdots w_{0n}], \quad \mathbf{w}_4^* = [w_{11} \cdots w_{mn}], \\
 \Psi_{x1}^* &= [0], \quad \Psi_{x2}^* = [\psi_{x10} \cdots \psi_{xm0}], \quad \Psi_{x3}^* = [\cdots 0 \cdots], \quad \Psi_{x4}^* = [\psi_{x11} \cdots \psi_{xmn}], \\
 \Psi_{y1}^* &= [0], \quad \Psi_{y2}^* = [\cdots 0 \cdots], \quad \Psi_{y3}^* = [\psi_{y01} \cdots \psi_{y0n}], \quad \Psi_{y4}^* = [\psi_{y11} \cdots \psi_{ymn}], \quad (\text{A1})
 \end{aligned}$$

where

$$w_{m0} = \cos(2mx) + \frac{2m^2(-1)^m}{g_m} x^2,$$

$$\psi_{m0} = \frac{2m}{g_m} \sin(2mx) - \frac{4m^2(-1)^m}{g_m} x,$$

$$w_{0n} = \cos(2ny) + \frac{2n^2(-1)^n}{g_n} y^2,$$

$$\psi_{y0n} = \frac{2\beta n}{g_n} \sin(2ny) - \frac{4\beta n^2(-1)^n}{g_n} y,$$

$$w_{mn} = \frac{(-1)^{m+1} g_n (vm^2 + \beta^2 n^2)}{vm^2 g_{mn}} \cos(2mx) + \frac{(-1)^{m+1} g_n (m^2 + v\beta^2 n^2)}{v\beta^2 n^2 g_{mn}} \cos(2ny) \\ + \cos(2mx) \cos(2ny) + \frac{2(-1)^{m+n+1} \beta^2 n^2}{vg_{mn}} x^2 + \frac{2(-1)^{m+n+1} m^2}{v\beta^2 g_{mn}} y^2,$$

$$\psi_{xmn} = \frac{2(-1)^{m+1} g_n m (vm^2 + \beta^2 n^2)}{vm^2 g_n g_{mn}} \sin(2mx) \\ + \frac{2m}{g_{mn}} \sin(2mx) \cos(2ny) + \frac{4(-1)^{m+n} \beta^2 n^2}{vg_{mn}} x,$$

$$\psi_{ymn} = \frac{2(-1)^{m+1} g_n \beta n (m^2 + v\beta^2 n^2)}{v\beta^2 n^2 g_n g_{mn}} \sin(2ny) \\ + \frac{2\beta n}{g_{mn}} \cos(2mx) \sin(2ny) + \frac{4(-1)^{m+n} \beta m^2}{v\beta^2 g_{mn}} y \tag{A2}$$

and

$$g_m = 4m^2\gamma + 1; \quad g_n = 4\beta^2 n^2\gamma + 1; \quad g_{mn} = 4m^2\gamma + 4\beta^2 n^2\gamma + 1, \tag{A3}$$

in which $(m, n = 1, 2, \dots)$.

APPENDIX B

In equation (35), the elements of **a**, **D**, **E**, **F** are given by

$$\mathbf{a} = [\mathbf{a}_1 \quad \mathbf{a}_2 \quad \mathbf{a}_3 \quad \mathbf{a}_4]^T,$$

$$\mathbf{D} = \begin{bmatrix} \mathbf{D}_{11} & \mathbf{D}_{12} & \mathbf{D}_{13} & \mathbf{D}_{14} \\ \mathbf{D}_{21} & \mathbf{D}_{22} & \mathbf{D}_{23} & \mathbf{D}_{24} \\ \mathbf{D}_{31} & \mathbf{D}_{32} & \mathbf{D}_{33} & \mathbf{D}_{34} \\ \mathbf{D}_{41} & \mathbf{D}_{42} & \mathbf{D}_{43} & \mathbf{D}_{44} \end{bmatrix},$$

$$\mathbf{E} = \begin{bmatrix} \mathbf{E}_{11} & \mathbf{E}_{12} & \mathbf{E}_{13} & \mathbf{E}_{14} \\ \mathbf{E}_{21} & \mathbf{E}_{22} & \mathbf{E}_{23} & \mathbf{E}_{24} \\ \mathbf{E}_{31} & \mathbf{E}_{32} & \mathbf{E}_{33} & \mathbf{E}_{34} \\ \mathbf{E}_{41} & \mathbf{E}_{42} & \mathbf{E}_{43} & \mathbf{E}_{44} \end{bmatrix},$$

$$\mathbf{F} = \begin{bmatrix} \mathbf{F}_{11} & \mathbf{F}_{12} & \mathbf{F}_{13} & \mathbf{F}_{14} \\ \mathbf{F}_{21} & \mathbf{F}_{22} & \mathbf{F}_{23} & \mathbf{F}_{24} \\ \mathbf{F}_{31} & \mathbf{F}_{32} & \mathbf{F}_{33} & \mathbf{F}_{34} \\ \mathbf{F}_{41} & \mathbf{F}_{42} & \mathbf{F}_{43} & \mathbf{F}_{44} \end{bmatrix}, \quad (\text{B1})$$

where the row sub-matrix \mathbf{a}_m , which are given in equation (A1), contain, in the appropriate order, the corresponding unknown coefficients. The \mathbf{D}_{mn} , \mathbf{E}_{mn} and \mathbf{F}_{mn} are, respectively, the elastic stiffness, the initial stress stiffness and the consistent mass sub-matrix, and their elements are given as

$$\begin{aligned} (D_{mn})_{ij} = & \int_{-\pi/2}^{\pi/2} \int_{-\pi/2}^{\pi/2} \left[\frac{\partial(\psi_{xm}^*)_i}{\partial x} \frac{\partial(\psi_{xn}^*)_j}{\partial x} + \beta^2 \frac{\partial(\psi_{ym}^*)_i}{\partial y} \frac{\partial(\psi_{yn}^*)_j}{\partial y} \right. \\ & + v\beta \left(\frac{\partial(\psi_{xm}^*)_i}{\partial x} \frac{\partial(\psi_{yn}^*)_j}{\partial y} + \frac{\partial(\psi_{ym}^*)_i}{\partial y} \frac{\partial(\psi_{xn}^*)_j}{\partial x} \right) \\ & + v_1 \left(\beta \frac{\partial(\psi_{xm}^*)_i}{\partial y} + \frac{\partial(\psi_{ym}^*)_i}{\partial x} \right) \left(\beta \frac{\partial(\psi_{xn}^*)_j}{\partial y} + \frac{\partial(\psi_{yn}^*)_j}{\partial x} \right) \\ & + \frac{1}{\gamma} \left((\psi_{xm}^*)_i + \frac{\partial(w_m^*)_i}{\partial x} \right) \left(\psi_{xn}^*_j + \frac{\partial(w_n^*)_j}{\partial x} \right) \\ & + \frac{1}{\gamma} \left((\psi_{ym}^*)_i + \beta \frac{\partial(w_m^*)_i}{\partial y} \right) \left((\psi_{yn}^*)_j + \beta \frac{\partial(w_n^*)_j}{\partial y} \right) + K_1 (w_m^*)_i (w_n^*)_j \\ & \left. + K_2 \left(\frac{\partial(w_m^*)_i}{\partial x} \frac{\partial(w_n^*)_j}{\partial x} + \beta^2 \frac{\partial(w_m^*)_i}{\partial y} \frac{\partial(w_n^*)_j}{\partial y} \right) \right] dx dy, \\ (E_{mn})_{ij} = & \int_{-\pi/2}^{\pi/2} \int_{-\pi/2}^{\pi/2} \left[\frac{\partial(w_m^*)_i}{\partial x} \frac{\partial(w_n^*)_j}{\partial x} + \chi\beta^2 \frac{\partial(w_m^*)_i}{\partial y} \frac{\partial(w_n^*)_j}{\partial y} \right] dx dy, \\ (F_{mn})_{ij} = & \int_{-\pi/2}^{\pi/2} \int_{-\pi/2}^{\pi/2} [\theta^2 (w_m^*)_i (w_n^*)_j + (\psi_{xm}^*)_i (\psi_{xn}^*)_j + (\psi_{ym}^*)_i (\psi_{yn}^*)_j] dx dy, \quad (\text{B2}) \end{aligned}$$

in which $m, n = 1, \dots, 4$; and the i, j is the index of the sub-matrices of \mathbf{w}_m^* , $\boldsymbol{\psi}_{xm}^*$ and $\boldsymbol{\psi}_{ym}^*$. Note that equations (B2) and (D2) can be expressed in explicit forms as a set of long equations but, for the sake of brevity, the detailed expression are not shown.

APPENDIX C

In equation (39),

$$\alpha_{13} = -\frac{\nu}{4(1+\nu)} \frac{S_{11}}{S_{33}},$$

$$S_{11} = 96\gamma\beta^6\lambda_y + 4\beta^4[24\gamma(\lambda_x + \lambda_y) + 6\lambda_y + \gamma(48K_2 - \pi^2K_1)] \\ + \beta^2[24(1+4\gamma)\lambda_x + 48(1+\gamma)K_2 - (1+8\gamma)\pi^2K_1] - (1+4\gamma)\pi^2K_1,$$

$$S_{33} = 24\beta^4(\lambda_x + \lambda_y) + 24\beta^2(1+\beta^2)K_2 - (1+\beta^4)\pi^2K_1,$$

$$\alpha_{11} = \frac{(1+4\gamma)(\nu+\beta^2)}{\nu h_1} \alpha_{13}, \quad \alpha_{12} = \frac{(1+4\gamma\beta^2)(1+\nu\beta^2)}{\nu\beta^2 h_1} \alpha_{13},$$

$$\alpha_{14} = -\frac{2\beta^2}{\nu h_1} \alpha_{13} - \frac{1}{2(1+\nu)}, \quad \alpha_{15} = -\frac{2}{\nu\beta^2 h_1} \alpha_{13} - \frac{1}{2\beta^2(1+\nu)},$$

$$\alpha_{21} = \frac{2(\nu+\beta^2)}{\nu h_1} \alpha_{13}, \quad \alpha_{23} = \frac{2}{h_1} \alpha_{13},$$

$$\alpha_{24} = \frac{4\beta^2}{\nu h_1} \alpha_{13} + \frac{1}{(1+\nu)}, \quad \alpha_{32} = \frac{2(1+\nu\beta^2)}{\nu\beta h_1} \alpha_{13},$$

$$\alpha_{33} = \frac{2\beta}{h_1} \alpha_{13}, \quad \alpha_{15} = -\frac{2}{\nu\beta^2 h_1} \alpha_{13} - \frac{1}{2\beta^2(1+\nu)},$$

$$h_1 = 1 + 4\gamma + 4\gamma\beta^2. \quad (C1)$$

APPENDIX D

In equation (40),

$$\tilde{\lambda}_q = \lambda_q + M^T[\gamma_{11} \cos(2x) + \gamma_{12} \cos(2y) + \gamma_{13} \cos(2x) \cos(2y) + \gamma_{14}x^2 + \gamma_{15}y^2 + \gamma_{16}],$$

$$\gamma_{11} = -\frac{1}{\gamma} [(4\gamma\lambda_x + \gamma K_1 + 4\gamma K_2 + 4)\alpha_{11} - 2\alpha_{21}],$$

$$\gamma_{12} = -\frac{1}{\gamma} [(4\gamma\beta^4\lambda_y + \gamma K_1 + 4\gamma\beta^2 K_2 + 4\beta^2)\alpha_{12} - 2\beta\alpha_{32}],$$

$$\gamma_{13} = -\frac{1}{\gamma} \{ [4\gamma\lambda_x + 4\gamma\beta^4\lambda_y + \gamma K_1 + 4\gamma(1+\beta^2)K_2 + 4(1+\beta^2)]\alpha_{13} - 2\alpha_{23} - 2\beta\alpha_{33} \},$$

$$\gamma_{14} = -K_1\alpha_{14}, \quad \gamma_{15} = -K_1\alpha_{15},$$

$$\gamma_{16} = \frac{1}{\gamma} [2(\gamma\lambda_x + \gamma K_2 + 1)\alpha_{14} + 2\beta^2(\gamma\beta^2\lambda_y + \gamma K_2 + 1)\alpha_{15} + \alpha_{24} + \beta\alpha_{35}] \quad (D1)$$

and in equation (43)

$$\begin{aligned}
 Q_m(t) &= \int_{-\pi/2}^{\pi/2} \int_{-\pi/2}^{\pi/2} \tilde{\lambda}_q(x, y, t) W_m(x, y) dx dy, \\
 I_m &= - \int_{-\pi/2}^{\pi/2} \int_{-\pi/2}^{\pi/2} [\theta^2 \hat{W}(x, y) W_m(x, y) + \hat{\Psi}_x(x, y) \Psi_{xm}(x, y) + \hat{\Psi}_y(x, y) \Psi_{ym}(x, y)] dx dy, \\
 K_m &= \int_{-\pi/2}^{\pi/2} \int_{-\pi/2}^{\pi/2} [\theta^2 (W_m(x, y))^2 + (\Psi_{xm}(x, y))^2 + (\Psi_{ym}(x, y))^2] dx dy. \tag{D2}
 \end{aligned}$$